



Evolution of novel tricyclic CRTh2 receptor antagonists from a (*E*)-2-cyano-3-(1*H*-indol-3-yl)acrylamide scaffold

Anja Valdenaire, Julien Pothier, Dorte Renneberg, Markus A. Riederer, Oliver Peter, Xavier Leroy, Carmela Gnerre, Heinz Fretz*

Actelion Pharmaceuticals Ltd, Gewerbstrasse 16, CH-4123 Allschwil, Switzerland

ARTICLE INFO

Article history:

Available online 25 December 2012

Keywords:

CRTh2
DP₂
Prostaglandin
Asthma
Rhinitis

ABSTRACT

(*E*)-2-(3-(3-(3-Bromophenyl)amino)-2-cyano-3-oxoprop-1-en-1-yl)-1*H*-indol-1-yl)acetic acid (**1**) was discovered in a HTS campaign for CRTh2 receptor antagonists. An SAR around this hit could be established and representatives with interesting activity profiles were obtained. Ring closing tactics to convert this hit series into a novel 2,3,4,5-tetrahydro-1*H*-pyrido[4,3-*b*]indole based CRTh2 receptor antagonist series is presented.

© 2012 Elsevier Ltd. All rights reserved.

Prostaglandin D₂ (PGD₂), a major metabolite of arachidonic acid, is predominantly involved in the physiological response to allergy. It is released at high concentration by immunoglobulin E activated mast cells upon allergen challenge¹ and was demonstrated to activate two G-protein coupled receptors (GPCRs), the classical DP₁ receptor and the recently discovered chemoattractant receptor-homologous molecule expressed on T-helper 2 cells (CRTh2 also known as DP₂) receptor.² CRTh2 activation leads to the recruitment of granulocytes and Th2 cells by chemotaxis³ to the inflammation site and has been in almost all cases demonstrated to be pro-inflammatory.^{4,5} Furthermore it is now well established that antagonizing selectively the CRTh2 receptor could be useful in the treatment of asthma and other inflammatory diseases such as allergic rhinitis.^{6–10} Herein, we describe the discovery of a novel chemotype series and its conversion into a new lead series, which eventually should deliver potent, highly selective CRTh2 antagonists for oral application.

As already described in a preceding publication,¹¹ our search for CRTh2 receptor antagonists started by screening about 80,000 GPCR biased compounds from our in-house compound collection by means of an intracellular Ca²⁺ liberation (FLIPR™, Molecular Devices) assay with HEK-293 cells stably expressing the human (*h*) CRTh2 receptor. This effort provided two distinct screening hits that could be confirmed as valuable starting points for a lead discovery program. The hit-to-lead evolution of 2-(2-((2-(4-chlorophenoxy)ethyl)thio)-1*H*-benzo[d]imidazol-1-yl)acetic acid, was discussed in an earlier publication.¹¹ A second hit, (*E*)-2-(3-(3-

(3-bromophenyl)amino)-2-cyano-3-oxoprop-1-en-1-yl)-1*H*-indol-1-yl)acetic acid (**1**, Fig. 1), was identified as a singleton and its potency to antagonize PGD₂ induced *h*CRTh2 receptor activation with an IC₅₀ = 0.6 μM was confirmed. Furthermore, **1** was shown to compete against [³H]PGD₂ for the *h*CRTh2 receptor with an IC₅₀ = 0.5 μM in a radioligand displacement assay.

A library of approximately 200 compounds with the general structure **2** (Fig. 1) was prepared in a semi-automated high-throughput mode in order to confirm that singleton **1** is a true hit belonging to a hit cluster, and to demonstrate a clear structure–activity relationship (SAR) within this cluster. Eventually, replacements for the structural alerts like the cyano group, the α-cyanoacrylamide motif, and the N-aryl amide bond should be envisaged in order to reduce the presumed toxicity potential.¹² The carboxylic acid of **1** was kept throughout this validation process since it was recognized as a common functionality to all endogenous prostanoids as well as many of the published prostanoid receptor agonists and antagonists.¹³

The synthetic access of such analogues is outlined in Scheme 1. Commercially available 1*H*-indole-3-carbaldehyde **3a**, accordingly R¹ substituted, was condensed with pyrrolidine in a Dean–Stark apparatus to form (*Z*)-3-(pyrrolidin-1-ylmethylene)-3*H*-indole, which then was N-alkylated with either ethyl bromoacetate (*n* = 1), ethyl 3-bromopropanoate (*n* = 2) or ethyl 4-bromobutanoate (*n* = 3). Knoevenagel condensation of indolium bromide **4** with *tert*-butylcyanoacetate provided cyanoacrylate **5**.¹⁴ Literature precedence suggests that stereo-controlled *E*-selectivity in the formation of **5** relies on steric effects of the bulky carboxylate versus the less bulky cyano.¹⁵ The Knoevenagel condensation provided exclusively *E*-configured α-cyanoacrylate analogues as confirmed by

* Corresponding author. Tel.: +41 61 565 6208; fax: +41 61 565 8901.
E-mail address: heinz.fretz@actelion.com (H. Fretz).

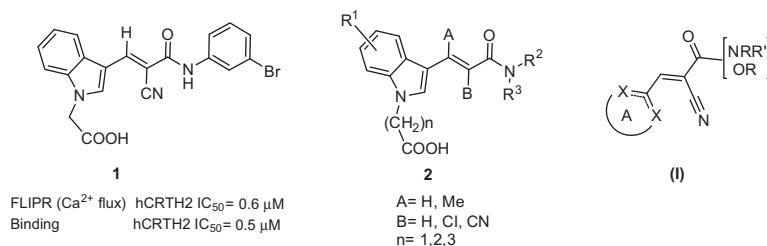
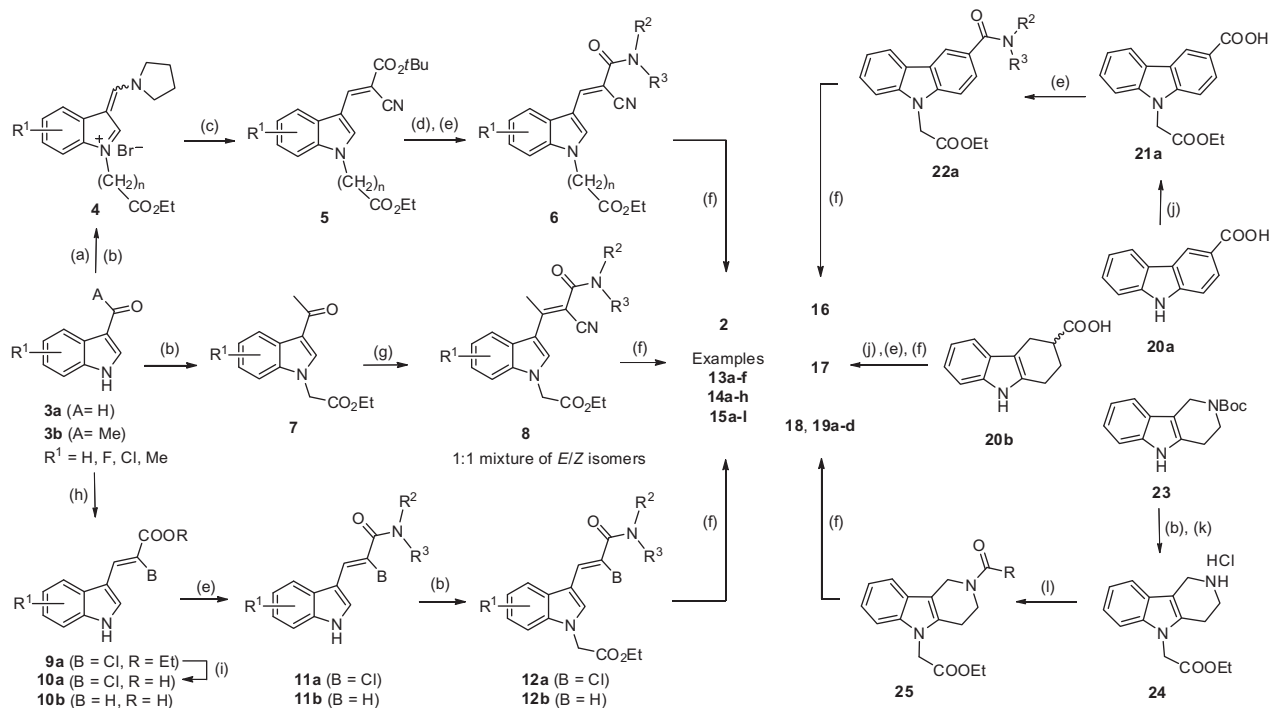


Figure 1. Structure of high-throughput screening hit **1**, general formula **2** indicating investigated positions to establish an SAR, and query formula **(I)** employed for the data base search of the Cambridge Crystallographic Data Centre (CCDC).



Scheme 1. Reagents and conditions: (a) pyrrolidine, toluene, reflux (87%); (b) Br(CH₂)_nCO₂Et, acetone, reflux, rt (70–93%); (c) NCCH₂CO₂tBu, NaOEt, EtOH, CHCl₃, rt; (d) 50% TFA in CH₂Cl₂, (97%); (e) (COCl)₂, DMF (cat.), CH₂Cl₂ (quant.); then HNR²R³, DIEA, CH₂Cl₂, 0 °C to rt (48–73%); (f) 1 M aqueous NaOH in THF, rt, 15 min to 2 h (35–100%); (g) NCCH₂CONR²R³, NH₄OAc, AcOH, toluene, 110 °C, 1:1 mixture of *E/Z* isomers (33%); (h) CCl₃CO₂Et, CrCl₂, THF, *E* isomer (31%); (i) LiOH in H₂O/THF (81%); (j) BrCH₂CO₂Et, NaH, DMF, rt (53%); (k) 4 M HCl in dioxane, rt, overnight (88%); (l) RNCO, DIEA, DCM, rt, 5 h (80%); or RCOCl, TEA, DCM, 0 °C to rt (44–89%).

ROESY NMR experiments (data not shown). A data base search of the Cambridge Crystallographic Data Centre (CCDC) for compounds with the generic formula **(I)** yielded 82 X-ray crystal structures, 61 comprising the alkyl 3-aryl-2-cyanoacrylate and 21 the 3-aryl-2-cyanoacrylamide motif, respectively (Refcodes listed in [Supplementary Table S1](#)). All the structures displayed (*E*)-configured substitution of the α -cyanoacrylate double bond. The X-ray crystal structures revealed co-planarity of the double bond with ring A at C(3) of the acrylate moiety in all the cases where there is no substituent connected to the ring atom X. In particular, the recently published X-ray crystal structure of methyl (*E*)-2-cyano-3-(1*H*-indol-3-yl)acrylate (VEGMAW) displays co-planarity of the double bond with the adjacent indole ring.¹⁶ Hydrolysis of *tert*-butylester **5** with 50% TFA, and subsequent amide formation applying an acid chloride procedure gave **6**. Pure final compounds **13a–c**, **14a–h** and **15a–l** were obtained after saponification of ethyl ester **6** and preparative reverse-phase (RP) HPLC purification.

Alkylation of 1-(1*H*-indol-3-yl)ethanone **3b** with ethyl bromoacetate followed by the Knoevenagel condensation of **7** with 2-cyano-*N*-phenylacetamide gave a 1:1 mixture of (*E*)- and (*Z*)-**8**.¹⁵ This mixture was subjected to saponification of the ethyl ester. The free

acid **13d** (first eluting peak, *R*_t = 3.04 min) and the corresponding *Z* isomer (second eluting peak, *R*_t = 3.28 min) were separated by preparative RP-HPLC.¹⁷ *E* and *Z* configuration could be unequivocally assigned by 1D selective gradient NOESY NMR experiments (data not shown). As expected, unambiguous interactions between the amide proton and the hydrogen atoms of the methyl group were observed for **13d**, confirming *E* configuration, whereas no such interactions were detectable for the second isomer. At this stage of the project, no effort was made to further explore the A site by other than methyl substitution due to the lack of a satisfying stereocontrolled access to pure *E* isomers with geminal substitution at C(3).

A stereoselective Cr(II) mediated *Z*-olefination protocol provided ethyl (*Z*)- α -chloroacrylate **9a** as a single geometrical isomer by reacting **3a** with ethyl trichloroacetate.¹⁸ Alkaline ester hydrolysis gave the free carboxylic acid **10a** which was converted to amide **11a** using the acid chloride method. Alkylation with ethyl bromoacetate in the presence of Cs₂CO₃, saponification of ethyl ester **12a** followed by acidic work-up provided the final product **13e** as the free acid. The preparation of **13f** started with the amidation of commercially available (*E*)-3-(1*H*-indol-3-yl)-2-propenoic acid

(**10b**) with aniline. Subsequent N-alkylation of **11b** and deprotection of **12b** finally provided **13f**.

In an initial study the relevance of substituents A, B, and the length of the carboxylic acid bearing alkyl chain (CH₂)_n was investigated. The data are summarized in Table 1. In comparison with **13a**, a considerable decrease in potency was observed with longer alkane chains than methylene, for example, propionic acid **13b** (IC₅₀ = 5.9 μM) and butanoic acid **13c** (IC₅₀ = 2.6 μM) were 13 and six times less potent, respectively. As demonstrated with **13d**, no change in potency was caused if A represents a methyl group instead of hydrogen and no significant change in affinity was observed with **13e** where a chlorine atom is replacing α-cyano. However, if B represents hydrogen as in **13f** a tenfold drop in potency was observed, indicating the importance of a substituent B.

As depicted in Table 2, very potent antagonists were obtained with N,N-disubstituted **14a–h**. If compared with **13a** for example, an almost 30-fold increase in potency was achieved with N-methyl analogue **14a**. Large hydrophobic groups were beneficial for good hCRTh2 affinity. Within this study, the most potent antagonist **14h** was identified with an IC₅₀ = 7 nM. All of the compounds discussed so far were shown to act as full antagonists in the Ca²⁺ liberation (FLIPR) assay (data not shown).

Next, the effects of R¹ substituents at the indole core were investigated (Table 3). The positional scanning, whereupon one hydrogen atom was substituted with fluorine, chlorine, and methyl, each at C(4), C(5), C(6) and C(7) as outlined with **15a–i**, uncovered that such groups had a beneficial effect at positions C(4) and C(5) providing antagonists with an IC₅₀ between 5 and 10 nM (**15a, b, e, f, i, j**). Significantly less potent compounds were obtained if the same substituents were attached at C(6) and C(7). As demonstrated with **15g** and **15k**, chlorine or methyl at C(6) decreased the IC₅₀ by a factor >50.

In order to further evaluate the 2-cyano-3-(1H-indol-1-yl)acrylamide series, potent representatives were investigated with respect to their in vitro pharmacological, physicochemical, ADME and in vivo pharmacokinetic characteristics. Analog **14g** is presented in Table 4 as a representative example with an IC₅₀ = 14 nM. Human serum albumin (HSA, 0.5%) was added to the assay buffer in order to identify those antagonists that potentially retain potency under conditions where binding to blood proteins occurs. No SAR and no clear correlations with physico-chemical parameters could be established concerning this frequently observed plasma shift effect. So far, one might conclude that compounds with small and less hydrophobic NR²R³, clogP < 3 and a negative LogD_{7.4} tend to be less affected. No plasma shift was observed for **14g** (IC₅₀ = 10 nM). An antagonistic effect with an IC₅₀ = 54 nM was obtained for **14g** in the functional Ca²⁺ release assay. Finally, **14g** was shown to inhibit in a functional assay dose-dependently the shape change of human eosinophils (hESC) with an IC₅₀ = 160 nM.^{19,20}

No cross-selectivity with other prostanoid receptors like the human prostaglandin E₂ (PGE₂) receptor subtypes hEP_{1–4}, the human thromboxane A₂ (TXA₂) receptor TP₂, and DP₂, the other PGD₂ receptor was noticed. A DP₁/CRTh2 selectivity factor of >500 was found.

Table 1
hCRTh2 receptor binding IC₅₀ values of compounds **13a–f**

Compd.	A	B	n	hCRTh2 binding (buffer) IC ₅₀ (nM)
a	H	CN	1	430
b	H	CN	2	5900
c	H	CN	3	2600
d	Me	CN	1	510
e	H	Cl	1	560
f	H	H	1	4400

Table 2
hCRTh2 receptor binding IC₅₀ values of compounds **14a–h**

Compd.	R ²	R ³	hCRTh2 binding (buffer) IC ₅₀ ^a (nM)
a	Phenyl	Methyl	15
b	Phenyl	<i>n</i> -Butyl	20
c	Phenyl	Cyclohexyl	30
d	Phenyl	Phenylmethyl	30
e	Phenyl	2-Phenylethyl	10
f			60
g			14
h			7

^a All IC₅₀ values are reported throughout the article as mean of at least three experiments.

The low molecular weight (MW < 400) of **14g** and its measured LogD_{7.4} value of −0.4 gave rise to a compound with excellent solubility (>600 μg mL^{−1}) in buffered aqueous solution at neutral pH.

A low potential for drug–drug interactions was expected, since the IC₅₀ values of **14g** on three major relevant cytochrome P450 enzymes (CYP 2C9, 2D6, 3A4) were >10 μM. Stability in different media was assessed by incubating **14g** in rat and human plasma for up to 4 h, in simulated gastric fluid (SGF) for 1 h and in simulated intestinal fluid (SIF) for 4 h.²¹ Recovery of unchanged parent was determined by LC–MS. The elimination half-life (T_{1/2}) of **14g** in rat as well as in human plasma was >4 h, with respective 90% and 95% recovery of the parent compound after 4 h incubation time. After incubation in SGF for 1 h, more than 90% of unchanged parent **14g** was recovered, whereas after exposure in SIF for 4 h, less than 70% was detectable, indicating that the compound is not stable if exposed to the latter conditions for a longer time. Metabolic stability of **14g** was assessed with human liver microsomes (HLM) and with rat liver microsomes (RLM) as well as with rat hepatocytes (RHepa). Respective intrinsic clearance (Cl_{int}) values of 6 and 32 μL min^{−1} mg^{−1} protein in HLM and in RLM preparations were determined, indicating a low metabolic conversion potential. Also, a good metabolic stability was observed in RHepa with a Cl_{int} of 11 μL min^{−1} 10⁶ cells^{−1}.

An in vivo pharmacokinetic study was carried out with **14g** in Wistar rats at single intravenous and oral doses of 1 and 10 mg/kg, respectively (Table 4). After intravenous dosing, a low plasma clearance (CL) of 14 mL min^{−1} kg^{−1}, a short terminal half-life (T_{1/2}) of 1 h, and common to carboxylic acids, an expected low volume of distribution (V_{ss}) of 0.7 L kg^{−1} was determined.

An exposure (AUC_{0–last}) of 2200 ng h mL^{−1} was found after oral administration. The resulting oral bioavailability of only 18% could be attributed to incomplete absorption.

So far, a cluster around singleton **1** was generated and a SAR could be established with analogues displaying potencies in the single digit nM range. Due to the limited oral bioavailability not exceeding the 20% threshold, and due to the fact that the structural alerts mentioned at the beginning still were present, a scaffold hopping exercise was initiated with the goal to identify novel core structures devoid of these unwanted features. Consequently, the vicinal substituted double bond motif of the (*E*)-2-cyano-3-(1H-indol-3-yl)acrylamide series was thoroughly studied in a

Table 3
hCRTh2 receptor binding IC₅₀ values of compounds **15a–l**

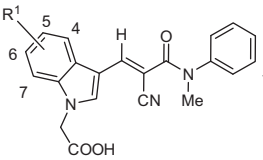
		Compd.	R ¹	hCRTh2 binding (buffer) IC ₅₀ (nM)	Compd.	R ¹	hCRTh2 binding (buffer) IC ₅₀ (nM)	Compd.	R ¹	hCRTh2 binding (buffer) IC ₅₀ (nM)
	a	F–C(4)	10	e	Cl–C(4)	5	i	Me–C(4)	10	
	b	F–C(5)	10	f	Cl–C(5)	7	j	Me–C(5)	7	
	c	F–C(6)	45	g	Cl–C(6)	290	k	Me–C(6)	690	
	d	F–C(7)	100	h	Cl–C(7)	50	l	Me–C(7)	140	

Table 4
Physicochemical, in vitro pharmacological and ADME, and in vivo pharmacokinetic characteristics of representative **14g** and new lead structure **19d**

		14g	19d			14g	19d
<i>Pharmacological properties</i>				<i>Physicochemical properties</i>			
hCRTh2 Bdg. (buffer)	IC ₅₀ (nM)	14	17	MW	(Da)	385	334
hCRTh2 Bdg. (0.5% HSA)	IC ₅₀ (nM)	10	15	LogD _{7.4}		–0.4	–1.2
hCRTh2 (Ca ²⁺ flux)	IC ₅₀ (nM)	54	170	Solubility in			
hESC (plasma)	IC ₅₀ (nM)	160	110	Water (pH 4.6) ^b	(μg mL ⁻¹)	17	64
hDP ₁ (PGD ₂ binding)	IC ₅₀ (μM)	8.2	>10	Buffer pH 4	(μg mL ⁻¹)	7	515
hEP _{1–4} ^a	IC ₅₀ (μM)	>10	>10	Buffer pH 7	(μg mL ⁻¹)	670	810
hTP ₂ (Ca ²⁺ flux) ^a	IC ₅₀ (μM)	>25	>25	Stability in		93	100
				SGF (parent after 1 h)	(%)	68	100
				SIF (parent after 4 h)	(%)		
<i>In vitro ADME properties</i>				<i>In vivo PK properties^c</i>			
Inhibition of				AUC _{0–last} (po)	(ng h mL ⁻¹)	2200	6300
CYP 2C9/2D6/3A4	IC ₅₀ (μM)	>10/>10/>10	>15/>50/>50	C _{max}	(ng mL ⁻¹)	213	600
Stability in plasma:				CL	(mL min ⁻¹ kg ⁻¹)	14	4.6
T _{1/2} rat/human	(h)	>4/>4	>4/>4	T _{1/2}	(h)	1	2.3
(% parent, 4 h)		(90/95)	90/90	V _{ss}	(L kg ⁻¹)	0.7	0.5
CL _{int} (HLM)/(RLM)	(μL min ⁻¹ mg ⁻¹ prot.)	6/32	5/<4	F	(%)	18	14
CL _{int} (RHepa)	(μL min ⁻¹ 10 ⁶ cells ⁻¹)	11	0.9				

^a hEP₂, hEP₄: PGE₂ binding; hEP₁, hEP₃: PGE₂ induced Ca²⁺ mobilization (FLIPR); hTP: U46619 induced Ca²⁺ mobilization (FLIPR).

^b In brackets: pH of final aqueous solution.

^c Oral administration (po) 10 mg/kg, intravenous (iv) 1 mg/kg as a solution in 20% propylene glycol/80% buffer, to three male Wistar rats, respectively.

conformational analysis using **13a** as a representative example. Obtained low energy conformations should then serve as a basis for the design of novel scaffolds. A hypothetical diene structure **II** reflecting the substitution pattern of the corresponding (*E*)-2-cyano-3-(1*H*-indol-3-yl)acrylamide motif is depicted in Figure 2 (A). Such a diene may adopt the *s-cis* or *s-trans* conformation. Generally, *s-trans* conformations of conjugated dienes are assumed thermodynamically more stable due to steric repulsion (1,3-allylic strain) between the two inside hydrogen atoms (or substituents) of the *s-cis* conformation. However, in the present example steric repulsion caused by the phenyl ring at C(4) forces the anticipated diene to adopt the *s-cis* conformation. A geometry and conformational energy analysis of **13a** was performed using semi-empirical PM6 and a restricted Hartree–Fock SCF calculation formalism (Pulay DIIS + Geometric Direct Minimization) with a 3-21G** basis set (Spartan '10). The result of this energy minimization calculation revealed that low energy conformations were predominantly *s-cis* configured whereas the *s-trans* conformers were classified as high energy conformations. The low energy conformation pictured in Figure 2 (B) displays co-planarity of the double bond with the adjacent indolyl ring. This is in agreement with the recently published X-ray crystal structure of methyl (*E*)-2-cyano-3-(1*H*-indol-3-yl)acrylate (VEGMAW).¹⁶

The calculated 3D structure of **13a** was used as a template for the molecular design of tricyclic core structures in order to lock the molecule in the *s-cis* conformation (Fig. 2(C)). By applying this ring closing tactic the respective carbazole **16**, 3,4-dihydro-1*H*-car-

bazole **17**, and tetrahydro-pyridoindole **18** were envisaged. Energy minimization calculations of the proposed tricyclic cores were performed and the low energy conformations were compared with **13a** (Supplementary Table S2). In general, the proposed molecules seem to exhibit a more bent and less planar shape than **13a**. Ultimately, the compounds were prepared according to established procedures (Scheme 1) from commercially available **20a**, **20b** and **23** in four steps, and tested in the above described CRTh2 binding and FLIPR assays. Carbazole **16** was found equipotent with **13a**, whereas fortuitously racemic **17** was three times more potent than **13a**, thus opening up another avenue to a novel and potent CRTh2 receptor antagonist series.²² Tetrahydro-pyridoindole **18** was found equipotent with **13a** (IC₅₀ = 430 nM). Although less potent than **17**, this achiral core was further explored with priority because analogues were easily accessible (Scheme 1) and no cumbersome chiral separation or development of an enantioselective synthesis was needed, as for example, for the production of 3,4-dihydro-1*H*-carbazole analogues of **17**. A preliminary SAR with a few analogues (Table 5) already indicated the potential of this new series, for example, replacing phenylamino in **18** with a more hydrophobic R (benzyl, **19a**, *n*-pentyl, **19c**) resulted in a twofold improvement in binding affinity, whereas a substantial loss was observed with **19b** bearing a small R (methyl). In comparison to **13a** and **18**, an unexpected 25-fold lower IC₅₀ value was measured for **19d** (R = phenyl) in the binding assay (IC₅₀ = 17 nM), and **19d** antagonized PGD₂ induced intracellular Ca²⁺ liberation with an IC₅₀ = 170 nM. Based on these intriguing potencies, it was decided

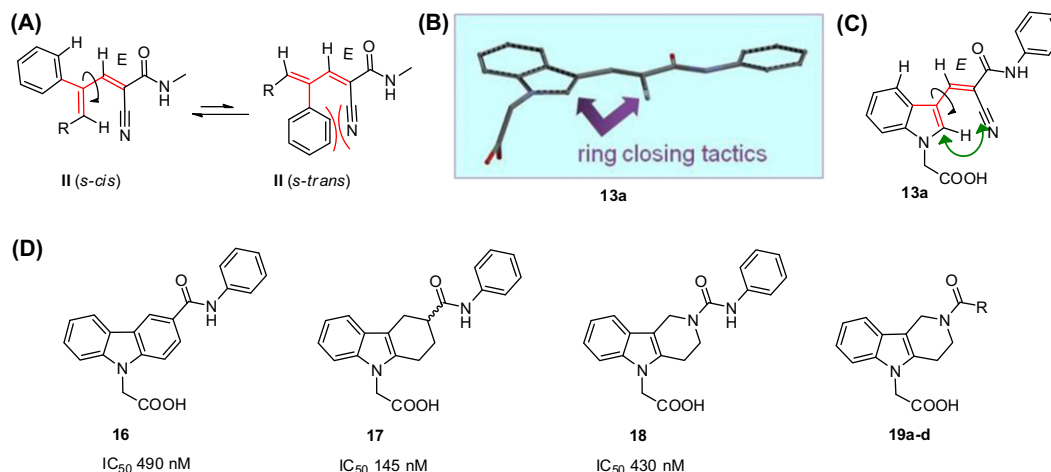


Figure 2. (A) Substituted diene **II** reflecting the (*E*)-2-cyano-3-(1*H*-indol-3-yl)acrylamide motif in its *s-cis* and *s-trans* conformation; (B) low energy conformation of structure **13a**, purple arrows indicate sites of ring closure; (C) molecular design: ring closing tactic (green arrow) locking the molecule in the *s-cis* conformation; (D) 'proof-of-concept' variants **16**, **17**, **18** and **19a-d** as envisaged from ring closing tactic.

Table 5
hCRTh2 receptor binding IC_{50} values of compounds **19a-d**

Compd.	R	hCRTh2 binding (buffer) IC_{50} (nM)
a	Benzyl	200
b	Methyl	1600
c	<i>n</i> -Pentyl	210
d	Phenyl	17

19

to fully characterize **19d** and to benchmark it with **14g** (Table 4). Comparable potency in the inhibition of the eosinophil shape change (IC_{50} = 110 nM) and high selectivity against the other prostanoid receptors were obtained. Improved PK characteristics, for example, a threefold higher exposure (AUC_{0-1ast} 6300 ng h mL⁻¹), a three times lower clearance (4.6 mL min⁻¹ kg⁻¹) and a prolonged $T_{1/2}$ (2.3 h) was found for **19d** in Wistar rats at single intravenous and oral doses of 1 and 10 mg/kg, respectively. The lack of obvious ADME liabilities (no CYP inhibition, low metabolic clearance), improved stability in SGF and SIF were the basis to further exploit **19d** as a novel drug-like lead structure, devoid of any structural alerts. Improving potency and oral bioavailability was the goal of a subsequent lead optimization program which would finally culminate in the selection of a clinical candidate (Fretz et al., in preparation).

In summary, we demonstrated the validation and characterization of a screening hit series. Attempts to eliminate assumed critical structural features led to the successful design of novel CRTh2 antagonist scaffolds. For example, the unexpected excellent properties of **19d** provided an excellent starting point for a lead optimization program.

Acknowledgements

The authors thank S. Koch, D. Lotz, A. Jonuzi, P. Risch, B. Butscha, J. Giller, B. Lack, S. Brand, for technical support, B. Capeleto for physico-chemical and Francois Le Goff for stability measurements in different solution media, R. Bravo, S. Delahaye, and H. Kletzl for

providing DMPK data, M. Holdener and K. Hilpert for supportive discussions, and J. Williams for proofreading the manuscript.

Supplementary data

Supplementary data associated with this article can be found, in the online version, at <http://dx.doi.org/10.1016/j.bmcl.2012.12.050>. These data include MOL files and InChIKeys of the most important compounds described in this article.

References and notes

- Murray, J. J.; Tonnel, A. B.; Brash, A. R. N. *Engl. J. Med.* **1986**, *315*, 800.
- Gervais, F. G.; Cruz, R. P.; Chateaneuf, A.; Gale, S.; Sawyer, N.; Nantel, F.; Metters, K. M.; O'Neill, G. P. *J. Allergy Clin. Immunol.* **2001**, *108*, 982.
- Hirai, H.; Tanaka, K.; Yoshie, O.; Ogawa, K.; Kenmotsu, K.; Takamori, Y.; Ichimasa, M.; Sugamura, K.; Nakamura, M.; Takano, S.; Nagata, K. *J. Exp. Med.* **2001**, *193*, 255.
- Pettipher, R. *Br. J. Pharmacol.* **2008**, *153*, S191.
- Kostenis, E.; Ulven, T. *Trends Mol. Med.* **2006**, *12*, 148.
- Pettipher, R.; Hansel, T. T.; Armer, R. *Nat. Rev. Drug Disc.* **2007**, *6*, 313.
- Chen, J. J.; Budelsky, A. L. *Prog. Med. Chem.* **2011**, *50*, 49.
- Burgess, L. E. *Annu. Rep. Med. Chem.* **2011**, *46*, 119.
- Schuligoi, R.; Sturm, E.; Luschig, P.; Konya, V.; Philipose, S.; Sedj, M.; Waldhoer, M.; Peskar, B. A.; Heinemann, A. *Pharmacology* **2010**, *85*, 372.
- Pettipher, R.; Hansel, T. T. *Prog. Respir. Res.* **2010**, *39*, 193. Karger: Basel.
- Pothier, J.; Riederer, M. A.; Peter, O.; Leroy, X.; Valdenaire, A.; Gnerre, C.; Fretz, H. *Bioorg. Med. Chem. Lett.* **2012**, *22*, 4660.
- Such structural alerts are not per se prohibitive for further drug development, as exemplified with approved Entacapone and Teriflunomide, both drugs comprising features related to this hit series.
- Hirata, T.; Narumiya, S. *Chem. Rev.* **2011**, *111*, 6209.
- Knoevenagel, E. *Chem. Ber.* **1894**, *27*, 2345.
- (a) Schwarz, M. J. *Chem. Soc., Chem. Commun.* **1969**, 212; (b) Zabicky, J. J. *Chem. Soc., Chem. Commun.* **1961**, 683.
- Sonar, V. N.; Parkin, S.; Crooks, P. A. *Acta Cryst.* **2006**, *E62*, o1077.
- Preparative reverse phase HPLC on a Atlantis Prep T3, 10 μ m, 30 \times 75 mm column; eluent A: acetonitrile, eluent B: water containing 0.5% formic acid; gradient: 10–90% A in 4 min.; flow rate: 75 ml/min.
- Barma, D. K.; Kundu, A.; Zhank, H.; Mioskowski, Ch.; Falck, J. R. *J. Am. Chem. Soc.* **2003**, *125*, 3218.
- Stubbs, V. E.; Schratl, P.; Hartnell, A.; Williams, T. J.; Peskar, B. A.; Heinemann, A.; Sabroe, I. *J. Biol. Chem.* **2002**, *277*, 26012.
- Sabroe, I.; Hartnell, A.; Jopling, L. A.; Bel, S.; Ponath, P. D.; Pease, J. E.; Collins, P. D.; Williams, T. J. *J. Immunol.* **1999**, *162*, 2946.
- Asafu-Adjaye, E. B.; Faustino, P. J.; Tawakull, M. A.; Anderson, L. W.; Yu, L. X.; Kwon, H.; Volpe, D. A. *J. Pharm. Biomed. Anal.* **2007**, *43*, 1854.
- Fecher, A.; Fretz, H.; Riederer, M. WO2006070325 (Actelion Pharmaceuticals Ltd, Switz.), PCT Int. Appl. (2006).